NASA/TP-2005-212856

Real-Time Stability Margin Measurements for X-38 Robustness Analysis

John T. Bosworth and Susan J. Stachowiak
NASA Dryden Flight Research Center
Edwards, California

February 2005

The NASA STI Program Office…in Profile

Since its founding, NASA has been dedicated to the advancement of aeronautics and space science. The NASA Scientific and Technical Information (STI) Program Office plays a key part in helping NASA maintain this important role.

The NASA STI Program Office is operated by Langley Research Center, the lead center for NASA's scientific and technical information. The NASA STI Program Office provides access to the NASA STI Database, the largest collection of aeronautical and space science STI in the world. The Program Office is also NASA's institutional mechanism for disseminating the results of its research and development activities. These results are published by NASA in the NASA STI Report Series, which includes the following report types:

- TECHNICAL PUBLICATION. Reports of completed research or a major significant phase of research that present the results of NASA programs and include extensive data or theoretical analysis. Includes compilations of significant scientific and technical data and information deemed to be of continuing reference value. NASA's counterpart of peer-reviewed formal professional papers but has less stringent limitations on manuscript length and extent of graphic presentations.

- TECHNICAL MEMORANDUM. Scientific and technical findings that are preliminary or of specialized interest, e.g., quick release reports, working papers, and bibliographies that contain minimal annotation. Does not contain extensive analysis.

- CONTRACTOR REPORT. Scientific and technical findings by NASA-sponsored contractors and grantees.

- CONFERENCE PUBLICATION. Collected papers from scientific and technical conferences, symposia, seminars, or other meetings sponsored or cosponsored by NASA.

- SPECIAL PUBLICATION. Scientific, technical, or historical information from NASA programs, projects, and missions, often concerned with subjects having substantial public interest.

- TECHNICAL TRANSLATION. English-language translations of foreign scientific and technical material pertinent to NASA's mission.

Specialized services that complement the STI Program Office's diverse offerings include creating custom thesauri, building customized databases, organizing and publishing research results…even providing videos.

For more information about the NASA STI Program Office, see the following:

- Access the NASA STI Program Home Page at ***http://www.sti.nasa.gov***

- E-mail your question via the Internet to help@sti.nasa.gov

- Fax your question to the NASA STI Help Desk at (301) 621-0134

- Telephone the NASA STI Help Desk at (301) 621-0390

- Write to:
  NASA STI Help Desk
  NASA Center for AeroSpace Information
  7121 Standard Drive
  Hanover, MD 21076-1320

NASA/TP-2005-212856

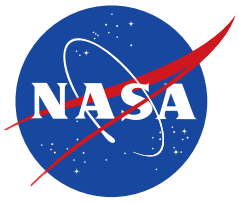

Real-Time Stability Margin Measurements for X-38 Robustness Analysis

John T. Bosworth and Susan J. Stachowiak
NASA Dryden Flight Research Center
Edwards, California

National Aeronautics and
Space Administration

Dryden Flight Research Center
Edwards, California 93523-0273

February 2005

Cover art: NASA Dryden Flight Research Center, photograph number EC99-45080-21.

NOTICE

Use of trade names or names of manufacturers in this document does not constitute an official endorsement of such products or manufacturers, either expressed or implied, by the National Aeronautics and Space Administration.

Available from:

NASA Center for AeroSpace Information (CASI)
7121 Standard Drive
Hanover, MD 21076-1320
(301) 621-0390

National Technical Information Service (NTIS)
5285 Port Royal Road
Springfield, VA 22161-2171
(703) 605-6000

ABSTRACT

A method has been developed for real-time stability margin measurement calculations. The method relies on a tailored-forced excitation targeted to a specific frequency range. Computation of the frequency response is matched to the specific frequencies contained in the excitation. A recursive Fourier transformation is used to make the method compatible with real-time calculation. The method was incorporated into the X-38 nonlinear simulation and applied to an X-38 robustness test. X-38 stability margins were calculated for different variations in aerodynamic and mass properties over the vehicle flight trajectory. The new method showed results comparable to more traditional stability analysis techniques, and at the same time, this new method provided coverage that is more complete and increased efficiency.

NOMENCLATURE

Symbols

CG	center of gravity
CRV	crew return vehicle
DFRC	Dryden Flight Research Center
dt	small change in time
e	base of natural logarithms
FFT	fast Fourier transformation
i	index of time domain data
j	square root of –1.0
k	index of frequency components in input excitation
m	total number of data points in time series
N_{cycles}	number of cycles of lowest frequency in one window
N_f	number of frequency components in excitation input
RTS	real-time stability
S	Laplace operator
t	time, sec
t_f	final time, sec
t_0	initial time, sec
TF	transfer function
T_{win}	total time (window length) to be processed, sec

T^*_{win}	total time (window length) to be processed rounded to nearest discrete time step, sec
U	time series of experimental excitation input applied to control effector actuator, deg
W_k	k^{th} discrete frequency in excitation, rad/sec
W_{min}	desired minimum frequency of excitation, cycles/sec
x	series of data in time domain
X	complex number of data transformed to frequency domain
Δt	time separation between points in measure data, sec
π	circumference of circle divided by two times its radius
ϕ_k	Schroeder phase shift to be applied at k^{th} frequency, rad
ω	frequency, rad/sec
ω_{HP}	frequency of high-pass filter, rad/sec

Functions

Im()	take imaginary part of complex number
$\log_{10}()$	base ten logarithm of number
Re()	take real part of complex number
$\tan^{-1}()$	arctangent of angle

INTRODUCTION

The conventional method for testing robustness of a space vehicle is to apply a Monte Carlo analysis. This involves varying some parameters, such as the aerodynamic, environmental, sensor, and/or mass properties of the vehicle; flying the vehicle trajectory; and assessing the percentage of success or failure. The success or failure criterion is derived from a general assessment that the mission goal was achieved. For successful instances, however, there is little indication of how close to failure each particular instance was. Adding a stability margin calculation to Monte Carlo analysis would provide a better indication of the true robustness of the vehicle.

The X-38 project developed a robustness test that combined some features of Monte Carlo analysis with conventional stability analysis. To accomplish this analysis combination, a set of test instances was selected with specific variations in aerodynamic and mass properties. Stability margin requirements were placed on each uncertainty instance. The stability margins were calculated using either a high-fidelity linear model or by frequency sweeps with the nonlinear simulation in a five-degree-of-freedom mode. This analysis was relatively time-consuming and relied on validated linear models or long duration frequency sweeps. In addition, since only two points along the trajectory were analyzed, there was no guarantee that the worst-case flight condition was addressed.

Therefore, to increase efficiency and cover more of the X-38 flight conditions, a new approach was developed that incorporates a real-time stability (RTS) margin calculation into the full six-degree-of-freedom X-38 nonlinear simulation. Results using the new method were compared to the original X-38 robustness test results. This report discusses this comparison, the improvements to the real-time stability margin measurement algorithm, and the benefits and weaknesses of this technique.

BACKGROUND

Linear stability analysis has been used extensively to test for vehicle robustness. The X-29 program used fast Fourier transformation (FFT) techniques to measure stability margins in flight (ref. 1). The pilot-generated frequency sweeps used for this in-flight measurement required long periods of stabilized flight (approximately one min).

Space vehicles such as the X-38 or X-34 are typically in a state of rapidly accelerating or decelerating flight. For vehicles with rapidly changing flight conditions, a tailored-forced excitation method was developed (ref. 2) to reduce the requirement for long periods of stabilized flight.

It was desired to incorporate the stability margin measurement into the Monte Carlo testing that is commonly used to test the robustness of space vehicles. By including a stability margin measurement into the Monte Carlo analysis, instances that may have survived but with very low margin, could be identified. In addition, sensitivity of the stability margin with respect to different parameters could be assessed. Conventional FFT methods combined with the large number of instances in a typical Monte Carlo run results in an impractical computational burden. Fortunately, a recursive Fourier transformation algorithm (ref. 3) can be used to dramatically reduce the computational requirements of the stability margin calculation. The subject of this report is this real-time (online) algorithm and its application to the X-38 Monte Carlo analysis.

X-38 PROGRAM BACKGROUND

The goal of the X-38 program was to demonstrate the technology required for the International Space Station's emergency crew return vehicle (CRV) (ref. 4). Based on the X-24A lifting body, five prototype vehicles were developed to demonstrate the CRV concept. These unmanned vehicles operate autonomously and use a steerable parachute, called a *parafoil*, for final descent and landing. Of the five X-38 vehicles, four were to be used only for atmospheric flight-testing and one was to be tested from space through reentry to landing. As these vehicles had no propulsion systems, they were to be carried to altitude under the wing of a B-52 airplane and released.

Vehicle 131R is one of the atmospheric flight test vehicles (fig. 1). The robustness analysis presented in this report was performed using the nonlinear simulation of vehicle 131R during free flight. Free flight (ref. 4) is the portion of flight after release from the B-52 airplane but before deployment of the parafoil. During free flight, the X-38 vehicle uses a dynamic inversion flight control system (ref. 5). A nominal free-flight trajectory lasts for 55 sec starting at Mach 0.75 at an altitude of 45,000 ft and ends at Mach 0.74 at an altitude of 28,000 ft (fig. 2).

As part of preflight certification, the X-38 vehicle 131R was required to pass a robustness test. A set of 20 test instances (20 uncertainty instances) was selected with specific parametric variations in aerodynamic and mass properties (table 1). Based on previous experience with lifting bodies and the space shuttle, values for three-sigma variation of these parameters were defined. The values in table 1 show the percent of this three-sigma change applied to each parameter. For each uncertainty instance, the vehicle stability margin was tested at high and low dynamic pressure flight conditions. The low dynamic pressure condition was defined as the point 8 sec into the free-flight trajectory. The high dynamic pressure condition was defined as 47 sec into the free-flight trajectory. The control system passed the robustness test if the margins at these two conditions were greater than 4-dB gain margin and 20-deg phase margin for all of the uncertainty test instances. The nominal instance required 6-dB gain margin and 45-deg phase margin.

Johnson Space Center performed this robustness analysis with a high-fidelity linear model. Dryden Flight Research Center (DFRC) independently verified the results. The DFRC analysis used an FFT approach with a nonlinear simulation. The simulation was limited to five-degree-of-freedom to maintain the altitude and Mach number during the relatively long duration frequency sweep excitation. Results from this FFT-based approach provide the basis for comparison of the new real-time technique.

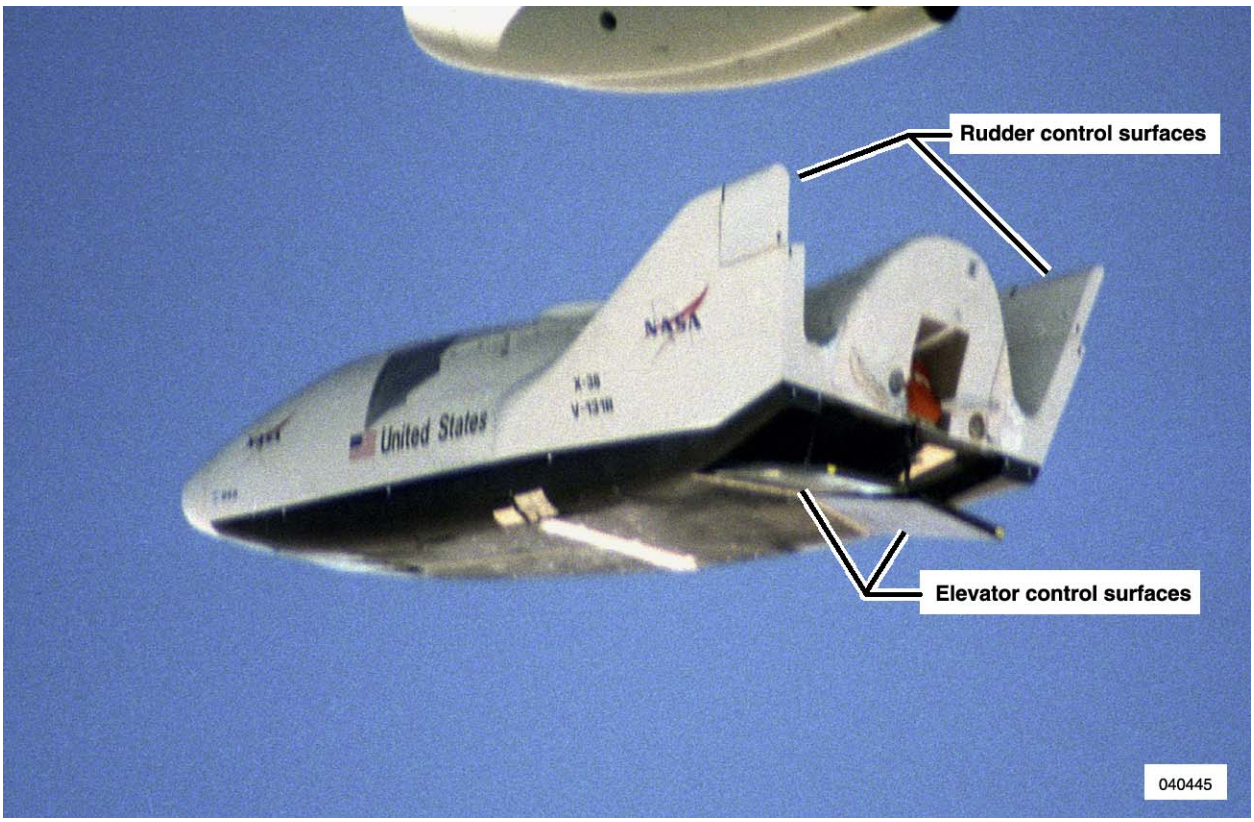

Figure 1. X-38 vehicle 131R.

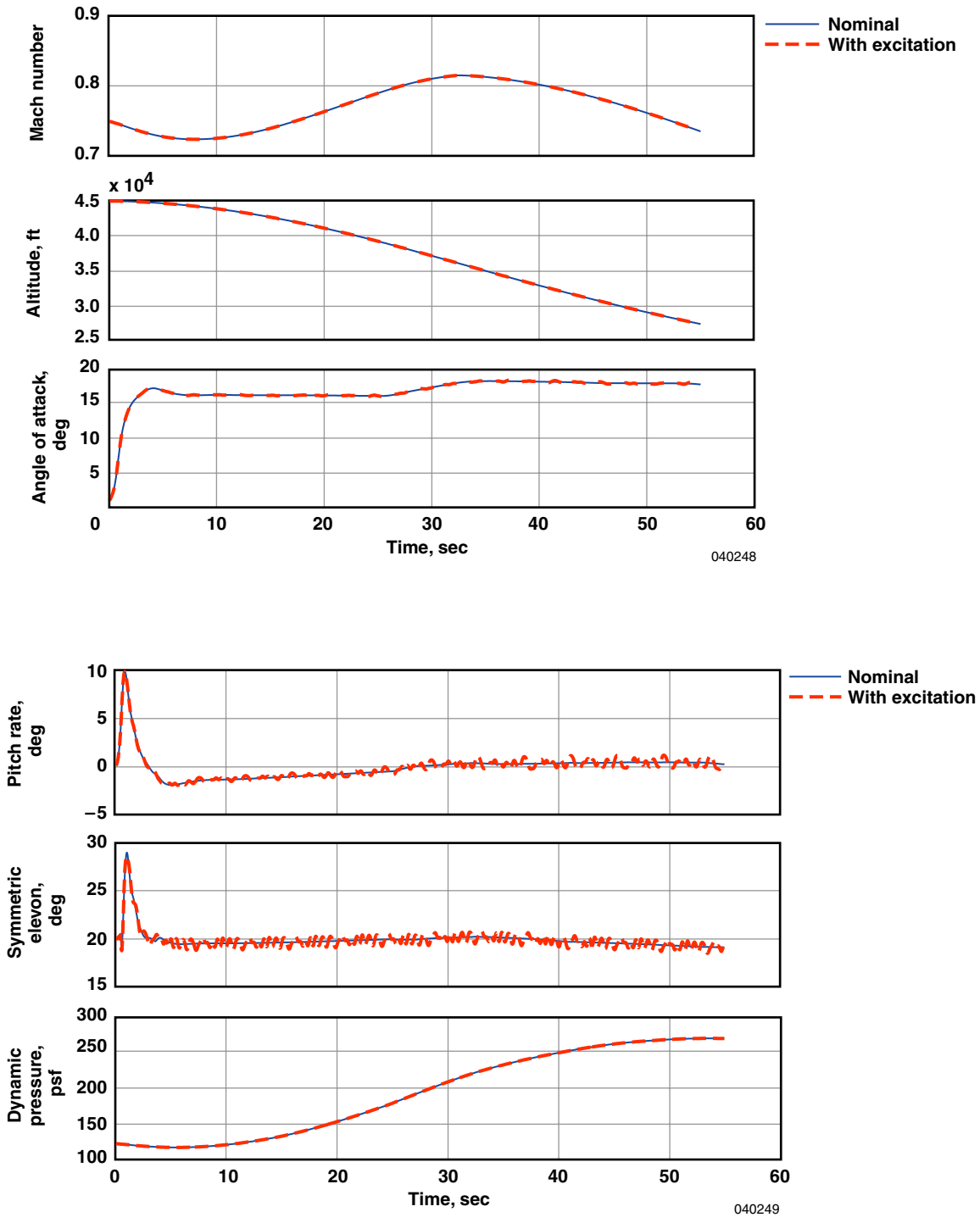

Figure 2. X-38 nominal free-flight trajectory.

Table 1. X-38 vehicle 131R uncertainty test instances.

Case name	1a	1b	1f	2a	2b	2f	3a	3b	3d	3e
Yaw due to beta	–66.7	–66.7	–66.7	–66.7	–66.7	–66.7	+66.7	+66.7	+66.7	+66.7
Roll due to beta	–66.7	–66.7	+66.7	+66.7	+66.7	+66.7	+66.7	+66.7	+66.7	+66.7
Roll due to aileron	–66.7	–66.7	–66.7	–66.7	–66.7	–66.7	–66.7	+66.7	–66.7	–66.7
Yaw due to aileron	–66.7	–66.7	–66.7	–66.7	–66.7	–66.7	–66.7	+66.7	–66.7	–66.7
Roll due to rudder	–66.7	+66.7	+66.7	+66.7	–66.7	–66.7	+66.7	+66.7	+66.7	–33.3
Yaw due to rudder	+66.7	–66.7	–66.7	–33.3	+66.7	+66.7	–33.3	–33.3	–33.3	+66.7
Side force due to beta	–66.7	–66.7	–66.7	–66.7	–66.7	–66.7	+66.7	+66.7	+66.7	+66.7
Side force due to rudder	0.0	0.0	0.0	0.0	0.0	0.0	0.0	0.0	0.0	0.0
Side force due to aileron	–66.7	–66.7	–66.7	–66.7	–66.7	–66.7	–66.7	+66.7	–66.7	–66.7
Pitching moment	–66.7	+66.7	+66.7	–66.7	+66.7	+66.7	–66.7	+66.7	+66.7	–66.7
Pitching moment due to elevon	0.0	0.0	0.0	0.0	0.0	0.0	0.0	0.0	0.0	0.0
Rolling moment	+66.7	+66.7	+66.7	+66.7	+66.7	+66.7	+66.7	+66.7	+66.7	+66.7
Yawing moment	+66.7	+66.7	+66.7	+66.7	+66.7	+66.7	+66.7	+66.7	+66.7	+66.7
Longitudinal CG change	forward	aft	aft	forward	aft	aft	forward	aft	aft	forward
Lateral CG change	right	right	right	right	right	right	right	right	right	right
Vertical CG change	up	down	up	up	down	up	up	down	down	up

Table 1. Concluded.

Case name	4a	4b	4d	5a	5b	6a	6b	7a	8a	8b
Yaw due to beta	+66.7	+66.7	+66.7	–66.7	–66.7	–66.7	–66.7	–66.7	–81.0	–66.7
Roll due to beta	–66.7	–66.7	–66.7	–66.7	–66.7	+66.7	+66.7	–66.7	0.0	+66.7
Roll due to aileron	+66.7	+66.7	+66.7	+66.7	+66.7	–66.7	–66.7	+66.7	0.0	0.0
Yaw due to aileron	+66.7	+66.7	+66.7	+66.7	–66.7	+66.7	+66.7	–66.7	0.0	0.0
Roll due to rudder	+66.7	–66.7	–33.3	+66.7	+66.7	–66.7	–66.7	–66.7	0.0	+66.7
Yaw due to rudder	–33.3	+33.3	+66.7	–66.7	–66.7	+66.7	+66.7	+66.7	0.0	–66.7
Side force due to beta	+66.7	+66.7	–66.7	–66.7	–66.7	–66.7	–66.7	–66.7	+81.0	+66.7
Side force due to rudder	0.0	0.0	0.0	0.0	0.0	0.0	0.0	0.0	0.0	0.0
Side force due to aileron	+66.7	+66.7	+66.7	+66.7	–66.7	+66.7	+66.7	–66.7	0.0	0.0
Pitching moment	–66.7	+66.7	+66.7	–66.7	+66.7	–66.7	+66.7	–66.7	0.0	0.0
Pitching moment due to elevon	0.0	0.0	0.0	0.0	0.0	0.0	0.0	0.0	0.0	0.0
Rolling moment	0.0	0.0	0.0	0.0	0.0	0.0	0.0	0.0	0.0	0.0
Yawing moment	0.0	0.0	0.0	0.0	0.0	0.0	0.0	0.0	0.0	0.0
Longitudinal CG change	forward	aft	forward	forward	aft	forward	aft	aft	none	none
Lateral CG change	right	right	right	right	right	right	right	right	none	none
Vertical CG change	up	down	down	up	down	up	down	up	none	none

REAL-TIME STABILITY MARGIN CALCULATION APPROACH

Reference 2 outlines a test technique to allow for measuring the stability of a vehicle or flight control system while minimizing the duration of the required input excitation. This report addresses how that technique was modified to be more compatible with real-time (online) processing. The major change was to incorporate a recursive Fourier transform algorithm to significantly reduce the computational requirements.

The real-time stability method uses a forced excitation applied to a control effector command. Measured time segments (windows) of the appropriate input and output variables are transformed to the frequency domain, and the open-loop frequency response is formulated. The resulting frequency response is used to calculate stability margins of the vehicle or flight control system. A time history of the stability margin can be obtained by repeating this calculation at each new time step. The time segment is moved by one time step for each new calculation, providing a sliding window of data.

Excitation Signal

The excitation signal used is a summation of cosine waves of specially selected frequencies. The frequency range selected is application specific and is further defined by the expected frequency at which the lowest stability margin occurs (crossover frequency). By carefully matching specific frequencies and the length of time segment (window length) being analyzed, problems associated with frequency leakage (ref. 2) are avoided, and good quality stability margin measurements are obtained.

Window Length

The lowest desired frequency and the number of cycles of that frequency determine the length of the time segment (window length) used for analysis. The stability margin calculation is a result of the dynamic response over the window length. A longer window length adds an effective delay of half the window length to the “real-time” calculation. Shorter window lengths are also desired for minimizing flight condition change during margin estimation. Window length may need to be increased, however, for better frequency resolution or to improve results in the presence of noisy data. In these cases, using multiple cycles at the lowest frequency lengthens process time.

The process time is computed from the number of cycles at the desired minimum frequency using:

$$T_{win} = \frac{1}{W_{min}(\text{cycles/sec})} \times N_{cycles} \tag{1}$$

This process time is rounded to the nearest discrete time step (Δt), which is usually the update rate of the flight control laws. The starting frequency is then adjusted to fit the actual window length. Higher frequencies whose cycle lengths fit evenly in the window defined above are selected using:

$$W_k(\text{rad/sec}) = 2\pi \times \frac{k}{T^*_{win}}, \text{ where } k \text{ is any positive integer.} \tag{2}$$

Phase Shifting

The top plot in figure 3 shows a typical excitation generated by a sum of cosines with no phase shifting of the individual frequencies. As suggested by Schroeder (ref. 6), the phase of each of the cosine waves was shifted before summing to reduce the peak factor of the excitation signal while maintaining the frequency content. The amount of phase shifting to apply to each of the discrete frequencies is computed from:

$$\phi_k = \frac{\pi k^2}{N_f} \tag{3}$$

The total excitation input is then obtained using the following equation:

$$U(t) = [\sum_{k=1}^{N_f} \cos(W_k \times t + \phi_k)] / N_f \tag{4}$$

The division by the total number of frequency components in excitation input (N_f) is used to normalize (scale) the amplitude of the resultant signal. The bottom plot on figure 3 shows an example of an excitation signal with Schroeder-phase shifting.

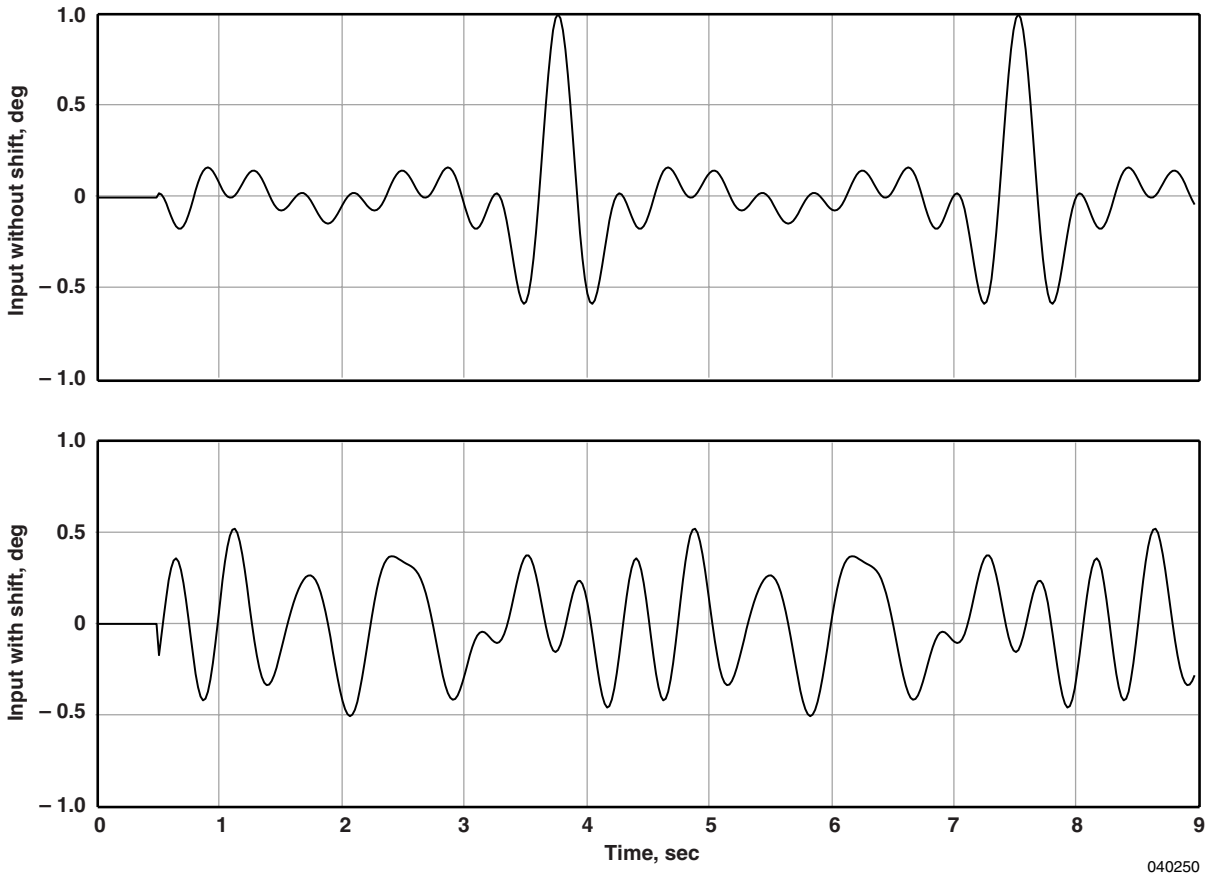

Figure 3. Effect of Schroeder-phase shifting on excitation signal.

Data Filtering

An important step in calculating a transfer function using FFT techniques is to de-trend the input and output time histories. The simplest way to perform this de-trend is to subtract the average of all the data points from each data point. This step can significantly improve the results when the data has a nonzero steady-state value (i.e., an elevator excitation with a nominal trim value of 5 deg). This method works well for a single frequency response calculation over a single time period. The objective is to calculate the frequency response at each time step using a moving window of data. To calculate an average at each time step would require storing many data points and computing an average at each time step.

A more efficient approach is to apply a high-pass filter to both the input and output data stream before doing the transformation to the frequency domain. The high-pass filter effectively removes the steady-state component of the time history data. Since the same filter is applied to both input and output, the transfer function relationship (ratio of output due to input) is preserved. The following simple high-pass filter was chosen:

$$\frac{\omega_{HP} S}{S + \omega_{HP}} \tag{5}$$

A value of ω_{HP} = 6 rad/sec seemed to work well. For ω_{HP} = 6 rad/sec, frequencies above 1.0 rad/sec are amplified and frequencies below 1.0 rad/sec are attenuated. This value worked for the X-38 vehicle where the lowest crossover frequencies are around 3 rad/sec, but this value might need adjustment for other vehicles with very low crossover frequencies.

Recursive Fourier Transformation

If the stability margin is calculated at each time step, using an FFT algorithm quickly becomes computationally prohibitive. Even if a Chirp-Z algorithm (ref. 2) is used with a limited number of frequencies, the calculations generally exceed the frame time. One solution is to run the calculation in the background, computing a margin at a slower update rate using leftover time spread over a number of computer timeframes.

Alternatively, a more efficient algorithm, such as the recursive Fourier transform, can be used for transformation to the frequency domain (ref. 3). This algorithm was used when performing the analysis on the X-38 vehicle. The increased algorithm efficiency allowed for stability margin calculation at each time step of the X-38 simulation.

The definition of the finite Fourier transform is:

$$X(\omega) = \int_{t_0}^{t_f} x(t)\, e^{-j\omega t}\, dt \tag{6}$$

Thus, the transformation from time domain to frequency domain is accomplished by integrating over the time segment of interest. When the sample time (Δt) is short compared to the period of the frequencies of interest, a simple Euler integration approximation can be used:

$$X(j\omega) = \Delta t \times \sum_{i=1}^{m} x(t_i) e^{-j\omega t_i} \tag{7}$$

Integration is required for each frequency of interest. With this transform, there is no restriction on which frequencies can be used, so the excitation frequencies can be used exactly.

To save computation time, it is not necessary to repeat this summation for each time segment. Instead, the discrete data sample points are stored in a buffer. At each new time step, the new data sample is added and the oldest data point is subtracted. In this manner, the process time is significantly reduced. This computational simplification comes at the cost of the memory required to save a potentially large number of data points in a buffer.

Computing Frequency Response

After the input and output have been transformed to the frequency domain, the two complex vectors are divided to create the open-loop transfer function:

$$TF(j\omega) = \frac{X_{output}}{X_{input}} \tag{8}$$

The elements of the complex vectors are then converted from complex number form to magnitude and phase form using the following:

$$phase = \tan^{-1} \frac{\mathrm{Im}(TF(j\omega))}{\mathrm{Re}(TF(j\omega))} \tag{9}$$

$$magdB = 20 \times \log_{10}\left(\sqrt{\mathrm{Re}(TF(j\omega))^2 + \mathrm{Im}(TF(j\omega))^2}\right) \tag{10}$$

The magnitude and phase of the transfer function can then be plotted against the frequency vector to form points on a Bode plot. Bode plot points calculated by the real-time stability method have compared well against Bode plots from the frequency sweep method as shown in figure 4. This result is a typical match for a linear system with good excitation.

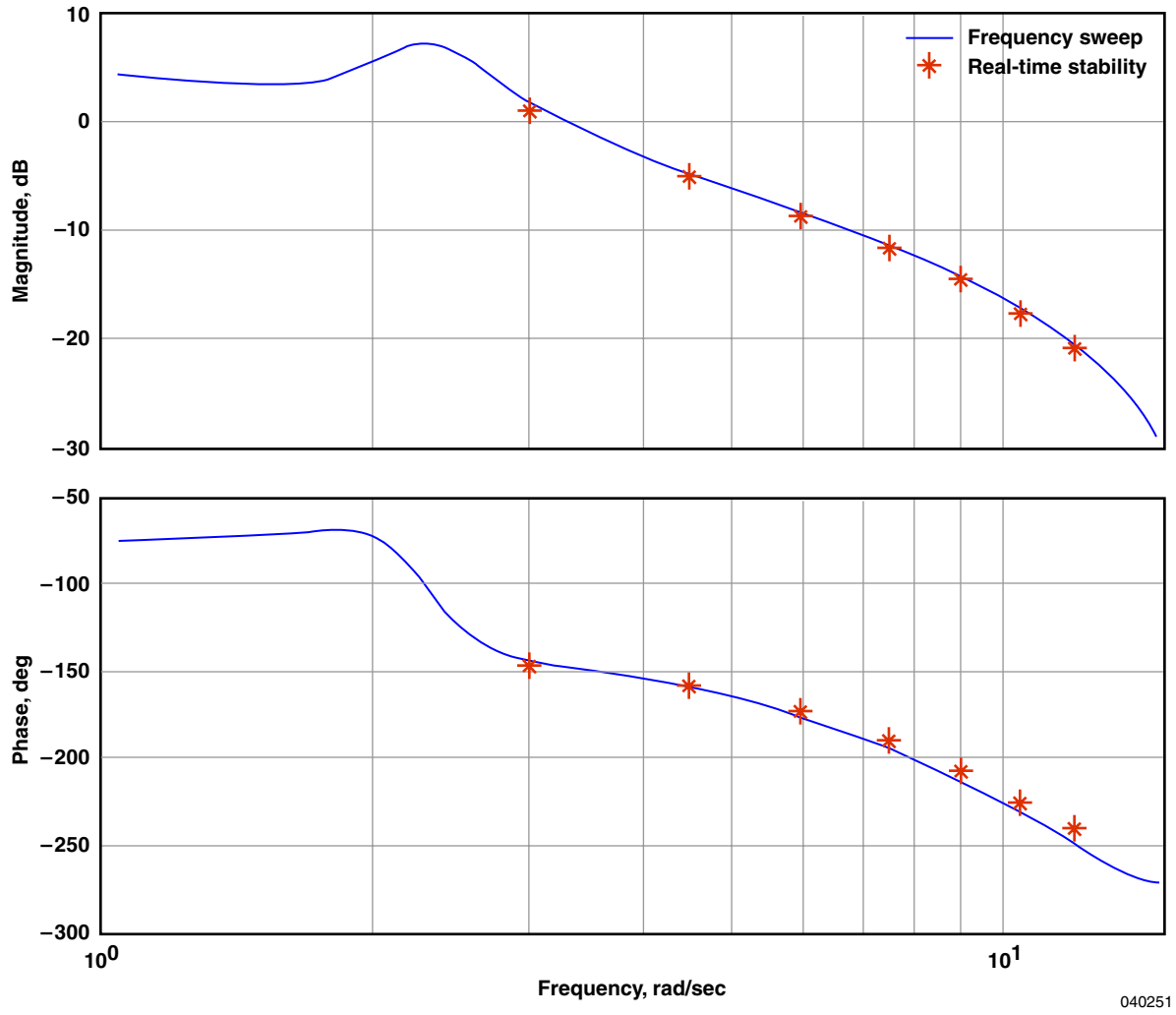

Figure 4. Comparison of frequency responses obtained from real-time stability and frequency sweep methods.

Stability Margin Calculation

Stability margins are calculated from the open-loop frequency response data using simple linear interpolation. Each point in the magnitude vector is compared with neighboring points to find two points that enclose the 0-dB crossover point. Linear interpolation is then used to estimate the gain crossover frequency and phase margin. To find the gain margin, points surrounding the –180-deg phase crossover are located. Linear interpolation is again used to estimate the actual phase crossover frequency and gain margin.

Errors introduced by linear interpolation are directly related to the frequency resolution of the frequency response points. The resolution can be improved by increasing the length of the process window. To achieve better resolution, either choose a lower value for the lowest desired frequency or increase the number of cycles at the lowest frequency.

APPLICATION TO X-38 ELEVATOR LOOP

The gain crossover for pitch axis of the X-38 vehicle typically occurs at around 3.5 rad/sec or higher. To obtain good margin calculations and sufficient frequency resolution, the following values were chosen:

$$W_{min} = 0.477 \text{ cycles/sec (3.0 rad/sec)} \tag{11}$$

$$N_{cycles} = 2 \tag{12}$$

The X-38 control system calculation rate is 25 times per sec. These parameters resulted in a time segment window length of 4.20 sec (105 points). An excitation signal was generated using the first nine frequencies with wavelengths that matched the time segment window. Table 2 shows these frequencies.

Table 2. Frequency content of X-38 excitation.

k	W_k, rad/sec
1	2.9920
2	4.4880
3	5.9840
4	7.4800
5	8.9760
6	10.4720
7	11.9680
8	13.4640
9	14.9600

Figure 2 shows a time history of a nominal X-38 trajectory. The vehicle is released from under the wing of a B-52 airplane at Mach 0.75 and an altitude of 45,000 ft. After an initial transient resulting from aerodynamic interaction with the B-52 airplane, the vehicle stabilizes at a commanded 16-deg angle of attack. At around 25 sec, the commanded angle of attack is changed to 18 deg. The vehicle flies for 55 sec of free flight before the parafoil deployment sequence is initiated. The X-38 stability robustness test was performed over this 55-sec period of free flight.

The dashed line on figure 2 also shows the same free-flight trajectory with the previously described excitation applied symmetrically to both elevators. The amplitude of the excitation was scaled to ±0.5 deg magnitude. The applied excitation provided small perturbations to pitch rate and angle of attack but did not significantly affect the vehicle trajectory.

The X-38 vehicle was flown on this trajectory with 20 different aerodynamic uncertainty variations (table 1). Figure 5 shows the resulting elevator loop phase and gain margins with their associated crossover frequencies. After approximately 10 sec, the calculated margins settle out to consistent reasonable results. Transients associated with release from the B-52 airplane corrupt results before 10 sec.

It should be noted that the stability margin is a calculation based on a time segment of data. In this case, the time segment (window) length is 4.2 sec. The time histories in figure 5 show a margin that is the result of the previous 4.2 sec of data. The margin is effectively delayed by half the window length. This provides another reason to use a shorter window length.

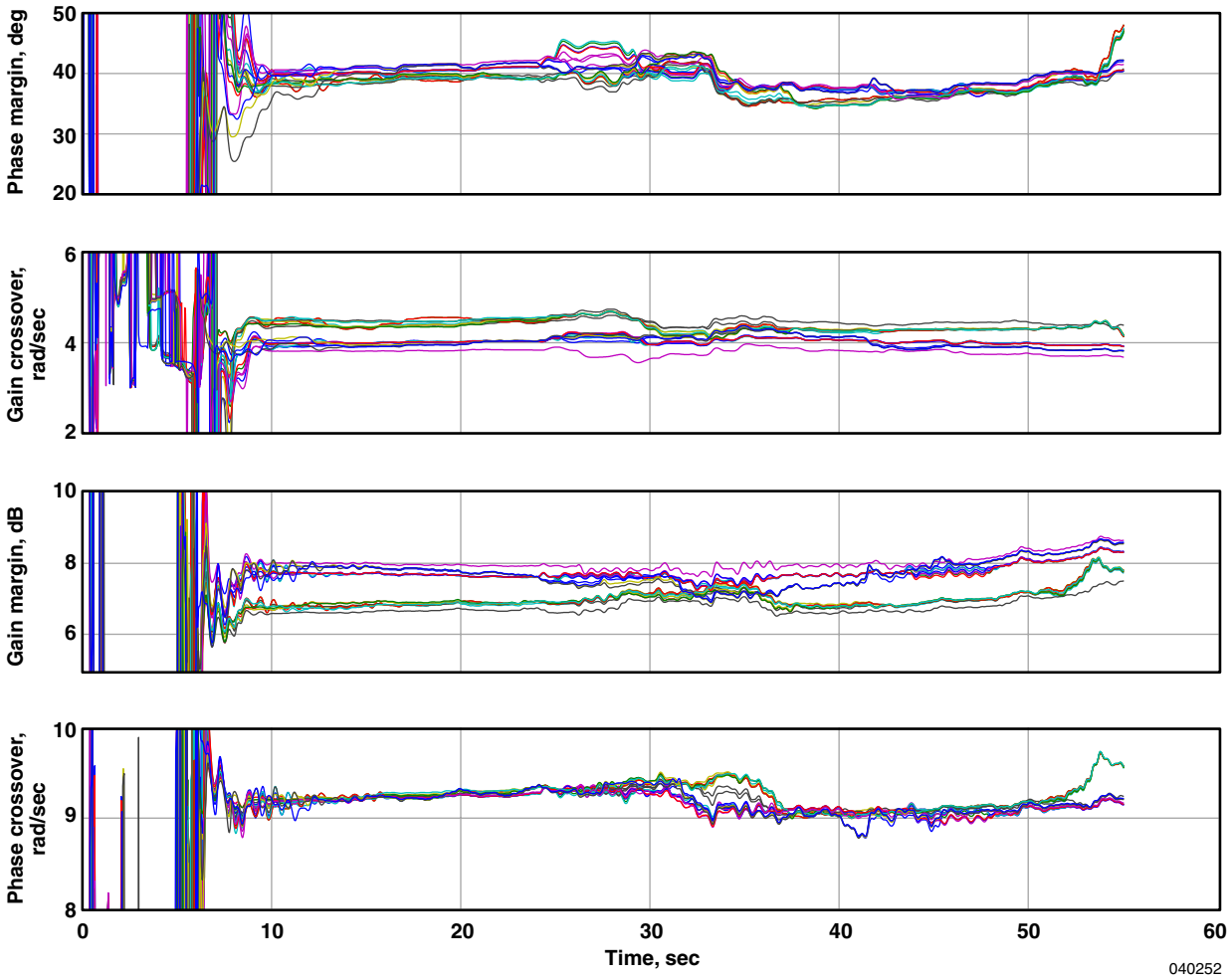

Figure 5. X-38 real-time stability margin calculation for elevator loop.

This figure 5 data show how stability changes with flight condition (and corresponding control system gain changes) and with varying uncertainties. The worst-case flight condition and uncertainty set can be quickly determined. For example, the uncertainty sets show two groupings with respect to gain margin. A look at the uncertainties shows that the group with the lower gain margins is associated with instances where pitching moment was increased by 66.7 percent.

To provide validation of these results, a comparison was made between the real-time stability method and more conventional frequency response methods using FFT. The flight condition obtained at 47 sec (high dynamic pressure) along the trajectory was chosen for this comparison. At 47 sec, the flight condition was "frozen" by putting the simulation into a five-degree-of-freedom mode. In this mode, the altitude and velocity states are not integrated. A relatively long duration (60 sec) frequency sweep was applied to the symmetric elevator command. Fourier transformation of the resulting response provided a calculation of the open-loop frequency response and the resulting stability margins. Figure 6 shows a comparison of the margins found by the real-time stability and the frequency sweep methods. In general, gain margins compared to within 0.15 dB and the phase margin was within 3 deg. Some of the phase margin difference is a result of interpolation errors caused by the lower frequency resolution of the RTS data.

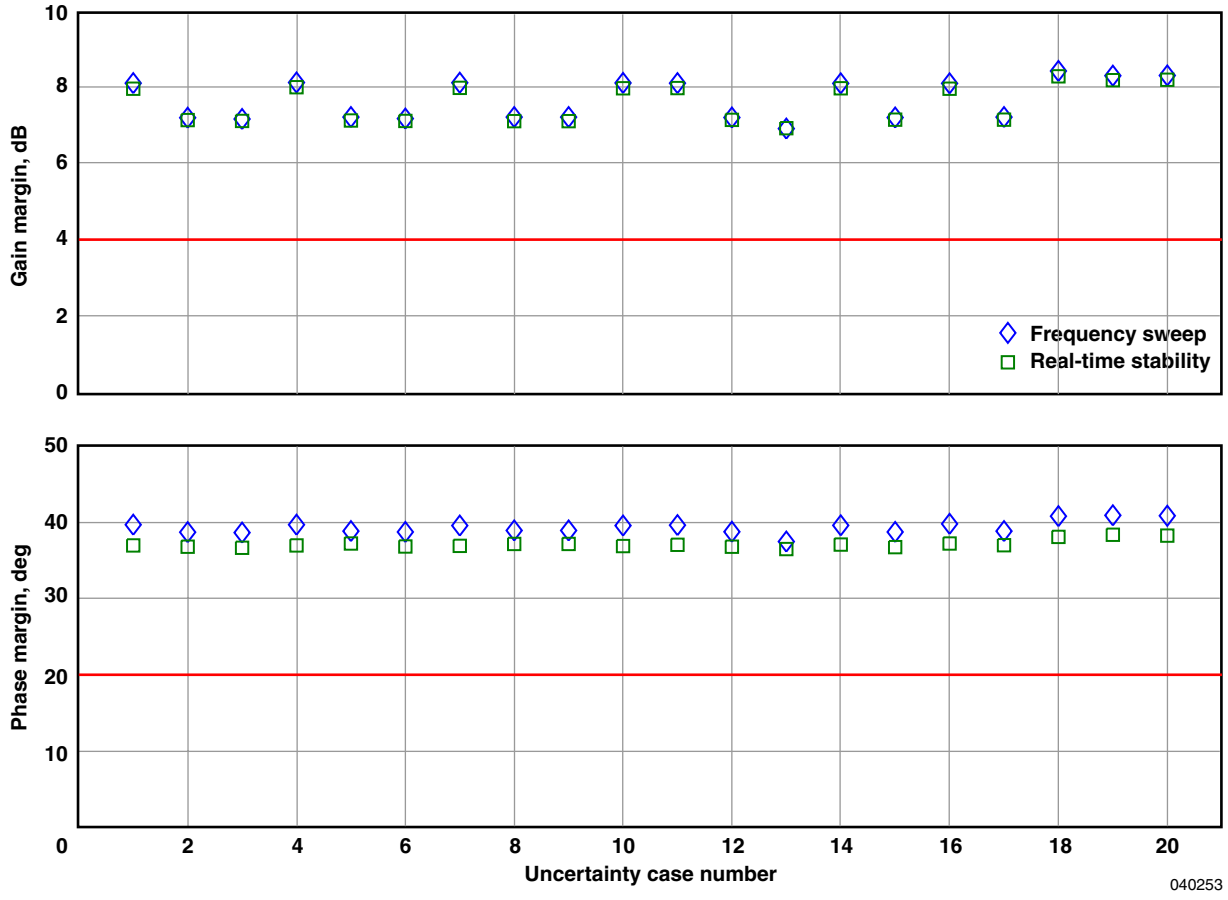

Figure 6. Elevator loop stability margins.

The simulation run time required to obtain the RTS results was much less than the time required to obtain the frequency sweep data. The RTS results can be obtained by running the simulation up to the time point of interest. For the frequency response results, the simulation was run up to the time point of interest and then run an additional 60 sec for the frequency sweep. In this case, the RTS results are for the entire trajectory, and the frequency sweep result is for only one time point. To obtain frequency sweep results for each time point would require 60 sec of simulation run time for each time point, plus the time to run the simulation until each point.

APPLICATION TO X-38 RUDDER LOOP

The stability margins associated with the rudder control loop were calculated using the same excitation as used for the elevator. Figure 7 shows the margins and crossovers as a function of time for the 20 uncertainty instances. The results for the rudder loop show less consistency than for the elevator loop. Some of the instances show significant variation with time. The expectation is that even though the flight condition might be changing, the vehicle dynamics should provide a relatively continuous and smooth change in behavior. Normally the stability margins should vary in a continuous and smooth manner.

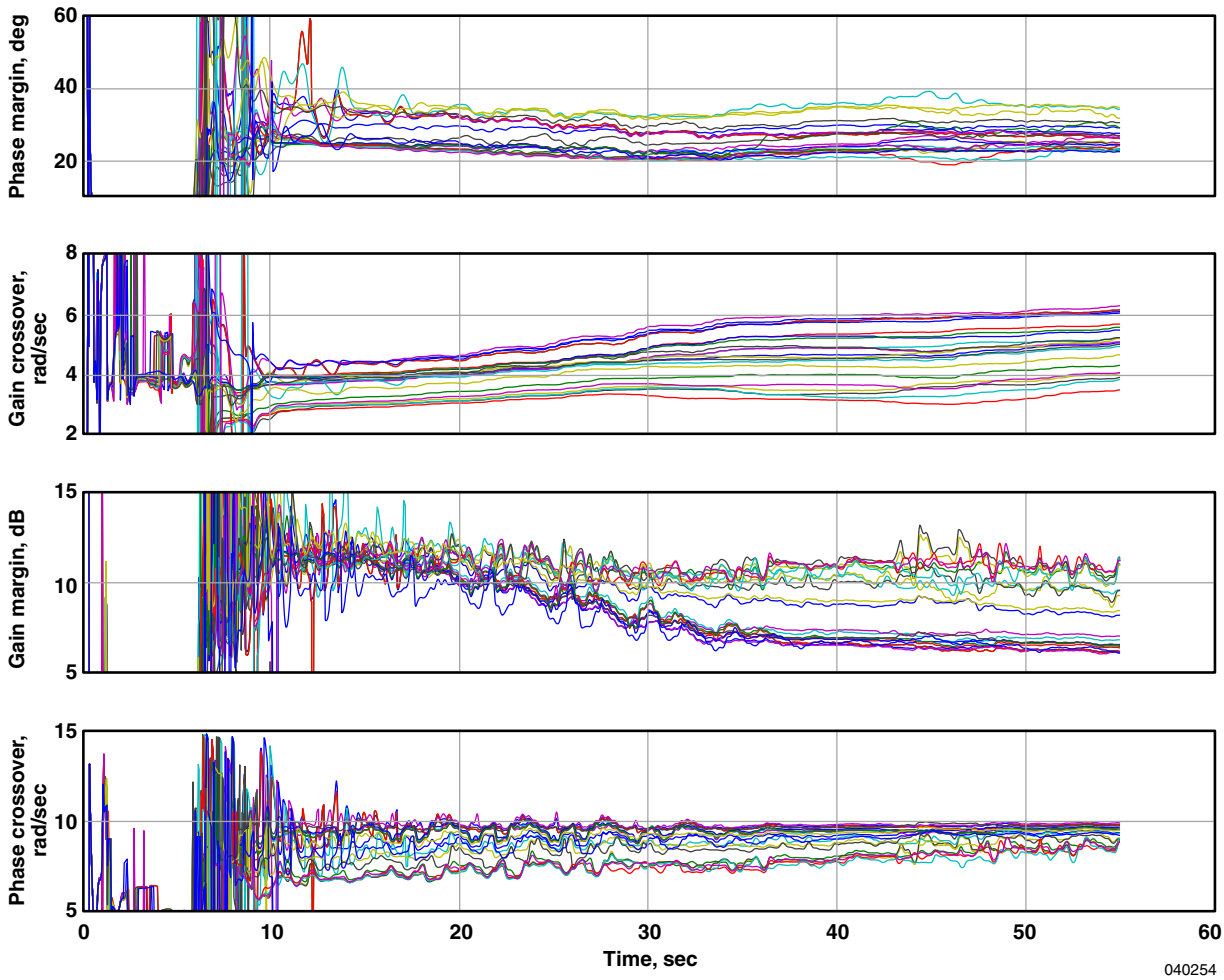

Figure 7. X-38 real-time stability margin calculation for rudder loop.

Closer examination of these results shows that relatively small variations in the frequency response caused these larger variations in gain margin. Figure 8 shows the rudder loop frequency response calculated (at each time step) over a two-sec period. This plot shows how the calculated frequency responses lie within a band. At the crossover frequency (8 rad/sec), the variations in phase angle were approximately 5 deg (approximately 10 msec). These fairly small variations in phase angle caused variations in the crossover frequency of approximately 1 rad/sec. Although the variations in the gain were fairly small (within 1 dB), the steepness of the curve results in gain margin variations of approximately 2 dB.

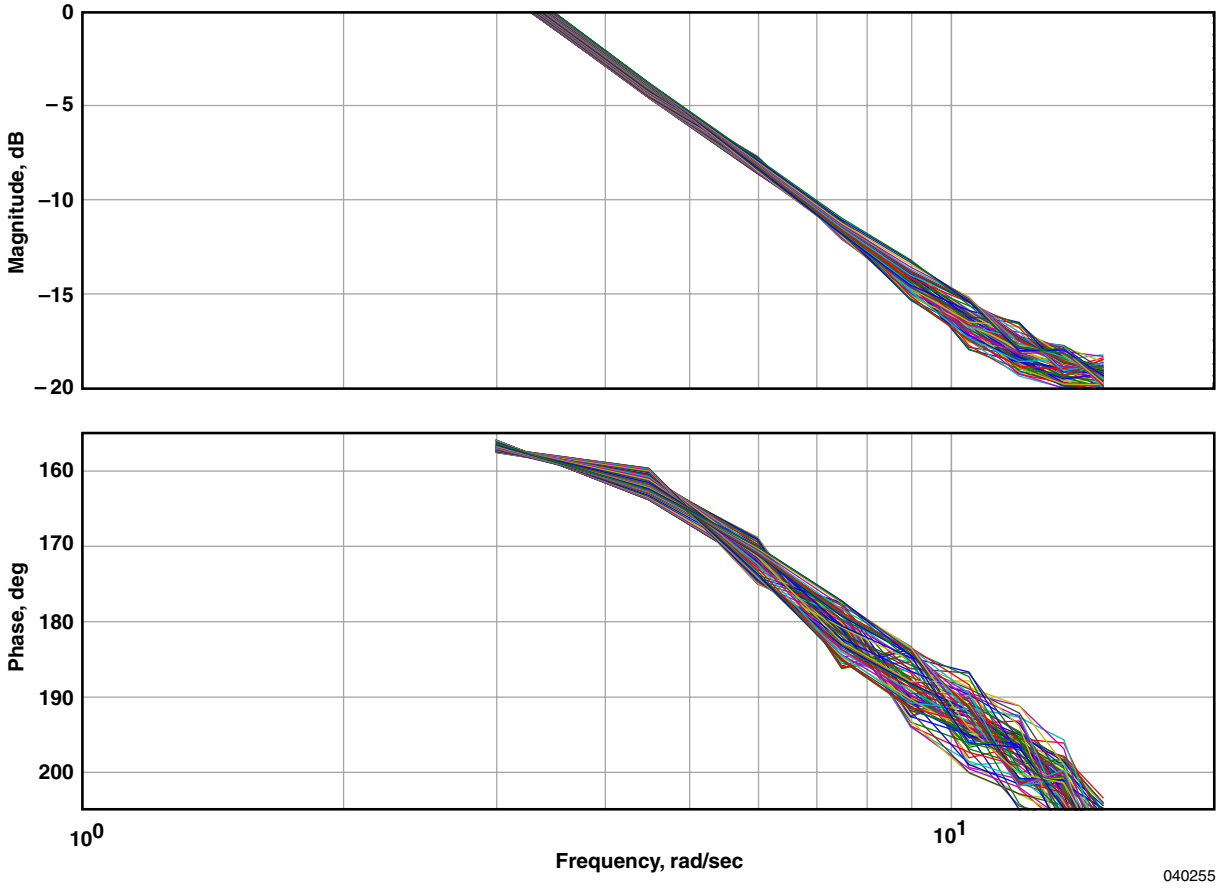

Figure 8. RTS results over two sec with large gain margin variations.

This erratic behavior shown in the rudder margin measurements is undesirable. For large Monte Carlo runs, regions of consistently low margin may be overlooked because attention is diverted to spurious peaks. Filtering the data can provide a clearer overall picture. The data from figure 7 was passed through the following filter:

$$\frac{1}{S+1} \tag{13}$$

Figure 9 shows the filtered margins and crossovers for the rudder loop. The filtered data provides a better means of looking for overall trends or for picking global margin minimums. The fact that the data were erratic and required filtering, however, may be a clue that there is some uncertainty in the margin measurement. For a well-behaved system, the system margins should change smoothly and relatively slowly with changes in conditions (i.e., dynamic pressure, angle of attack, etc.). Abrupt changes in margin should be investigated as potential problem areas.

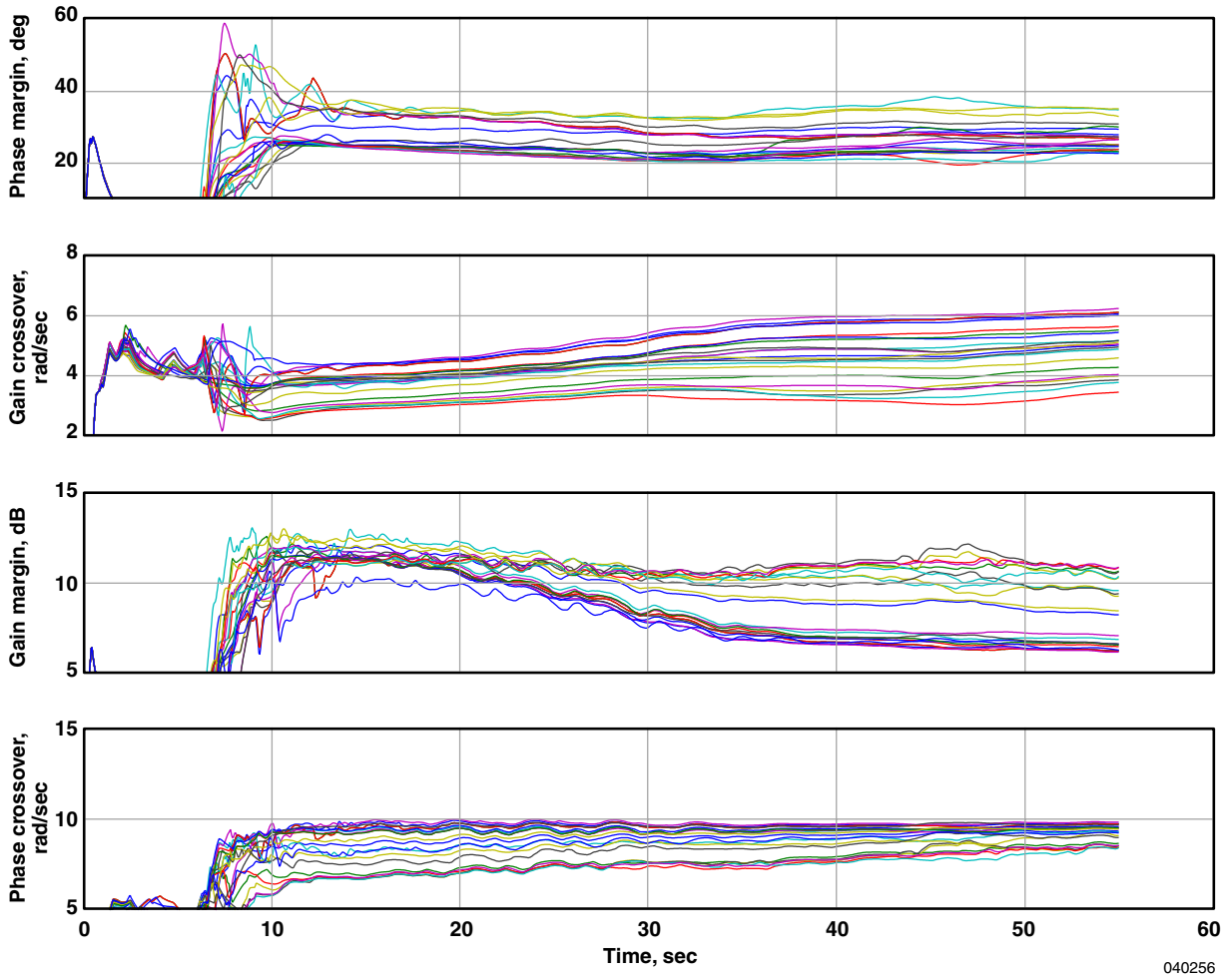

Figure 9. X-38 real-time stability margin calculation for rudder loop with filtering.

An estimation of the variation of the results can be obtained by simply calculating the difference between the filtered and unfiltered results.

$$\text{margin error estimation} = \text{abs}(\text{margin} - \text{filtered}(\text{margin})) \tag{14}$$

$$\text{crossover error estimation} = \text{abs}(\text{crossover} - \text{filtered}(\text{crossover})) \tag{15}$$

The mean and maximum error estimation can be used as part of the statistical analysis of Monte Carlo results. The mean of the error estimation can identify instances with less consistent results. Figure 10 shows the error estimation values for the rudder loop instances. These data show that the phase margin estimation has an error range of approximately ±1.5 deg, and the gain margin is within approximately ±1.0 dB. Figure 11 shows that the elevator loop gain margin errors were within ±0.25 dB; and the phase margin errors were mostly lower, with the exception of the peak errors of approximately 3 deg. These peaks (at roughly 25, 30, and 35 sec) correspond to changes in angle of attack and occur as the vehicle was in transition from 16-deg through 18-deg angle of attack.

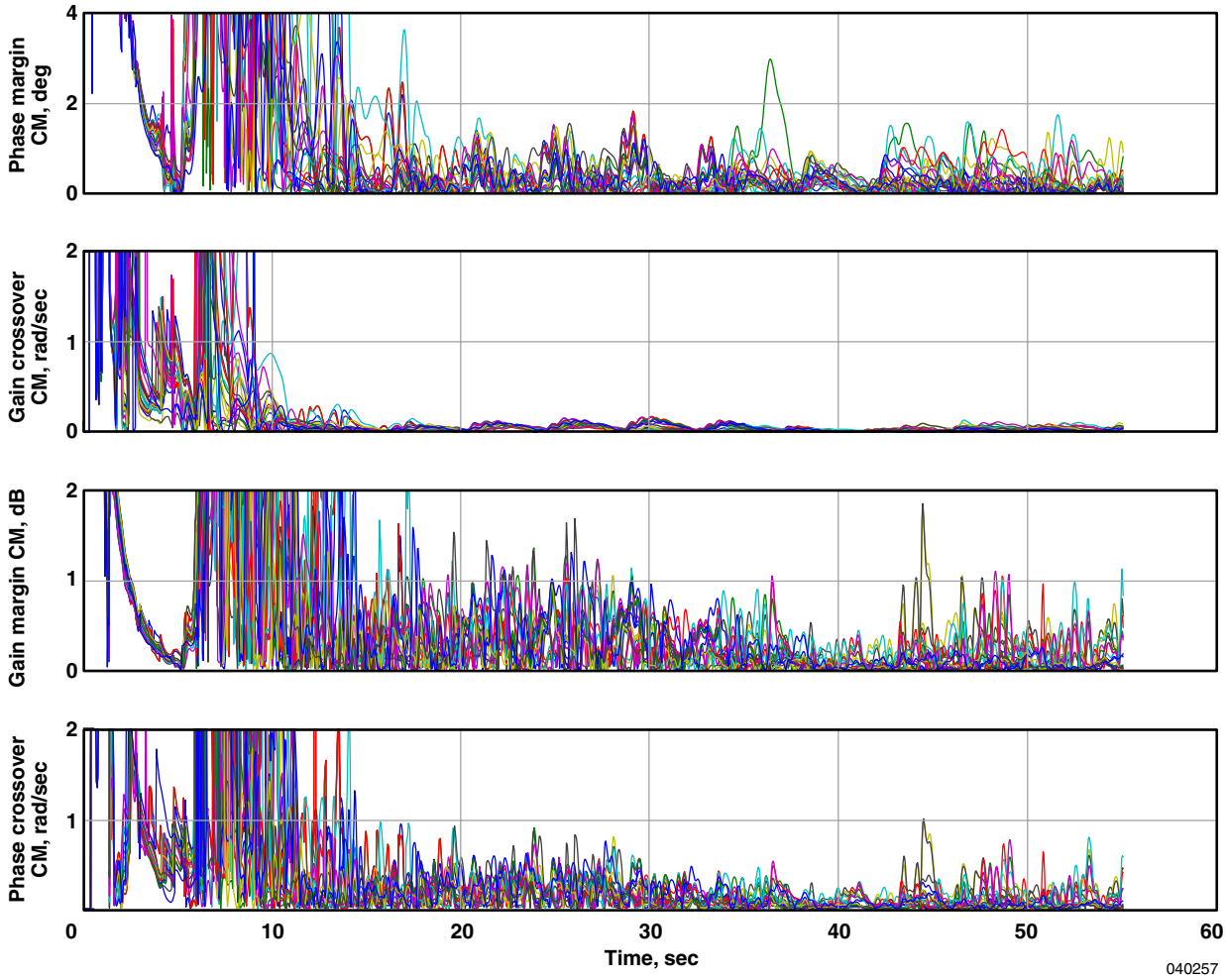

Figure 10. X-38 estimated errors for rudder loop.

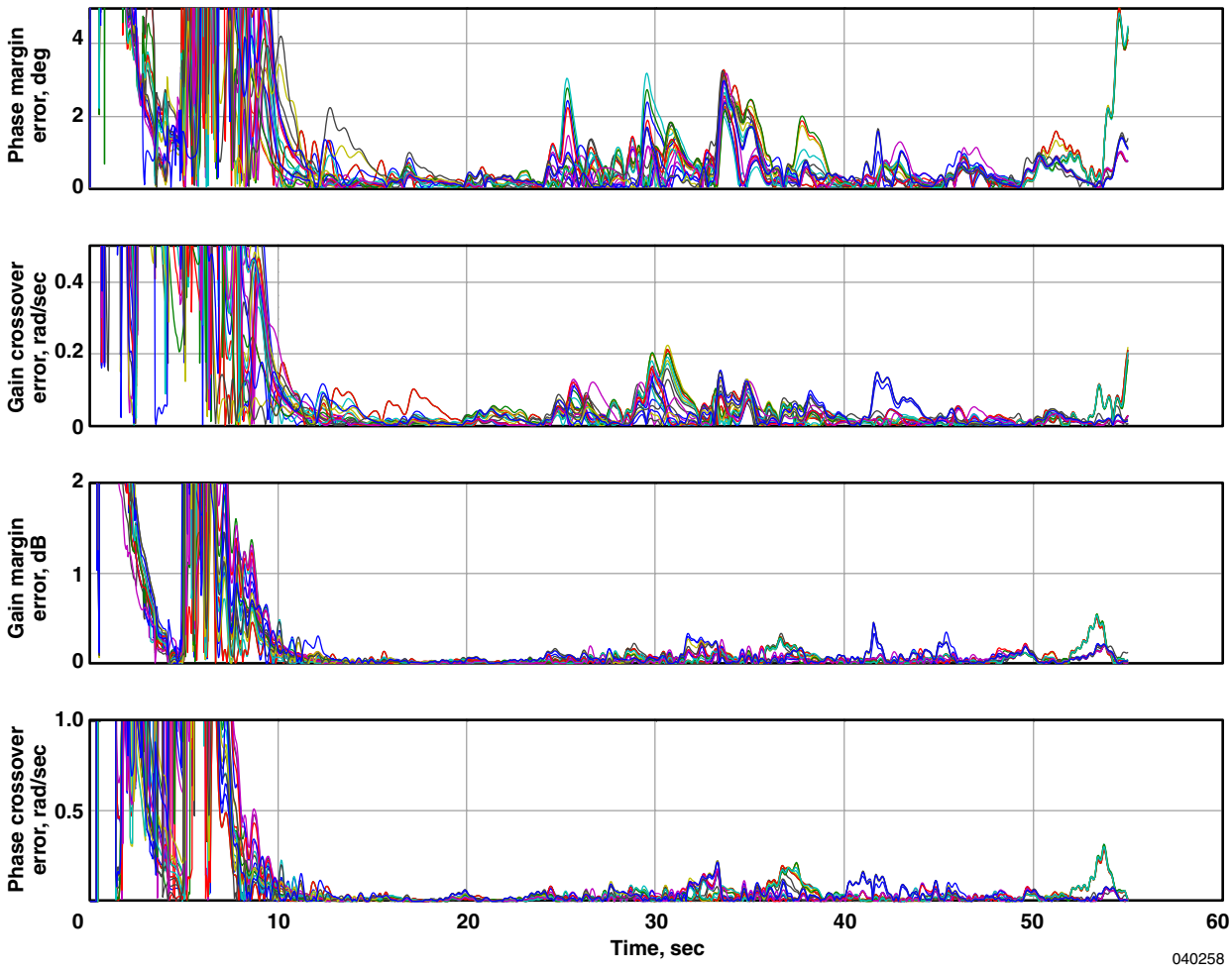

Figure 11. X-38 estimated errors for elevator loop.

SIMULTANEOUS MEASUREMENT OF ELEVATOR AND RUDDER MARGINS

To further increase efficiency, the elevator and rudder stability margins can be calculated simultaneously. This calculation is achieved by dividing the frequencies between the elevator and the rudder. The elevator gain and phase crossovers occur in the range from 3.5 through 4.5 rad/sec and 9 through 9.5 rad/sec respectively. The rudder gain and phase crossovers occur in the range from 3 through 6 rad/sec and 6.5 through 10 rad/sec respectively. The same discrete frequencies used in the previously-mentioned example were divided as shown in Table 3.

Table 3. Frequency content of excitation used for simultaneous inputs.

k	W_k, rad/sec	Control effector
1	2.9920	Elevator
2	4.4880	Rudder
3	5.9840	Elevator
4	7.4800	Rudder
5	8.9760	Elevator
6	10.4720	Rudder
7	11.9680	Elevator
8	13.4640	Rudder
9	14.9600	Elevator

The nominal trajectory (with no uncertainties) was flown with this excitation. Figure 12 shows the resulting stability margins obtained with simultaneous and separate excitations for the nominal instance. To better illustrate the differences, the data shown has not been filtered as was suggested in the previous section. Using simultaneous excitation produced results within 3 deg of phase margin and 0.5 dB of gain margin. Most of this difference is caused by interpolation with coarser data. Increasing the lowest frequency analyzed or the number of cycles of the lowest frequency could achieve better data resolution.

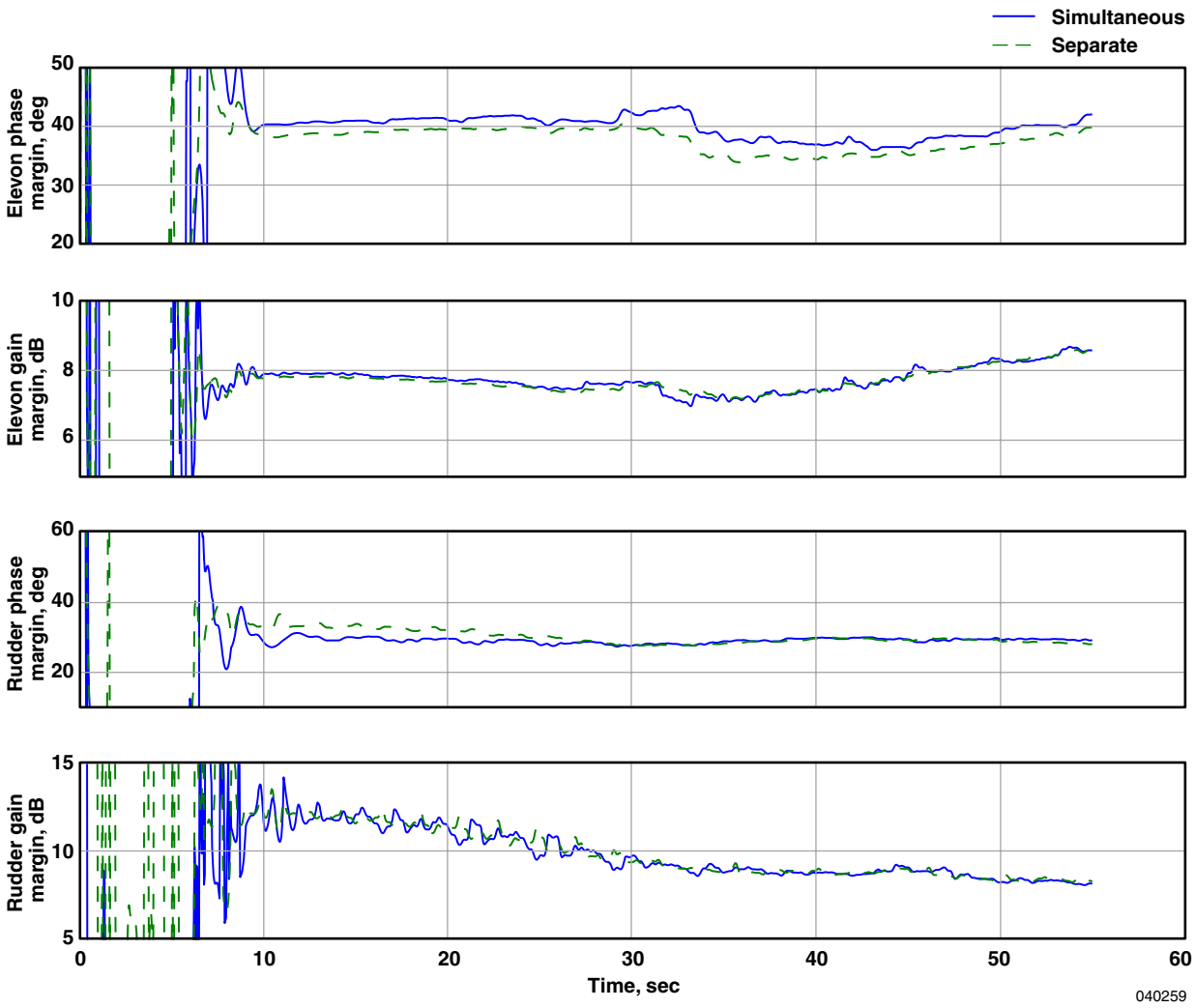

Figure 12. X-38 real-time stability margin calculation with simultaneous inputs.

INSTANCES WITH REDUCED STABILITY

The X-38 results were obtained with a mature control system that had good robustness characteristics. To show the RTS method with low stability, the rudder loop gain was varied from –6 dB through +8 dB. Figure 13 shows that the RTS method demonstrates good results even when neutral stability is reached. As the neutral stability point is reached, some variation in the results is apparent. At this point, the vehicle is reaching position saturation on the rudders, so some degradation in the linear relationship is expected. These data, however, show that the RTS method provides a good indication of an approaching instability.

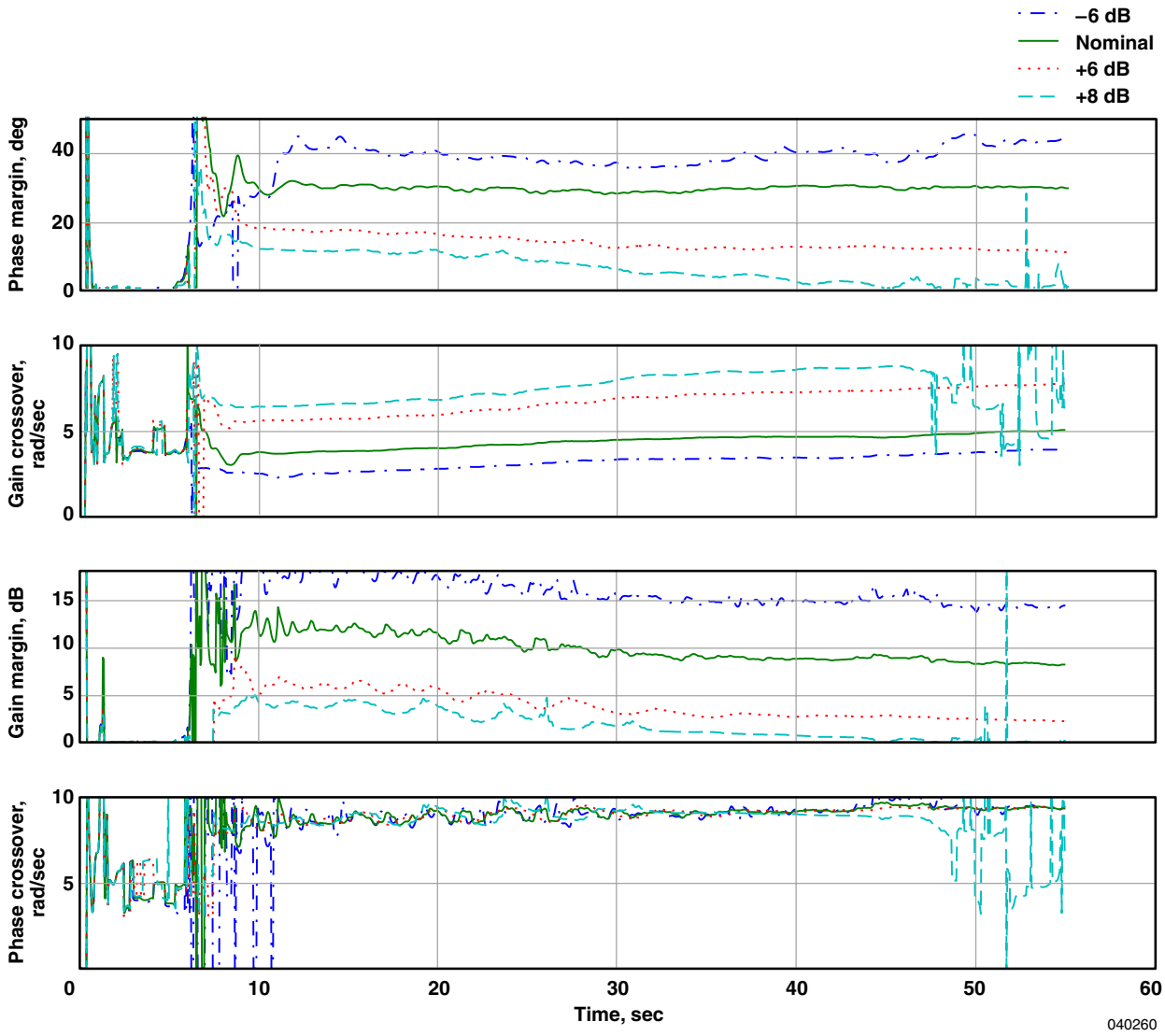

Figure 13. X-38 real-time stability margin calculation with variation in rudder loop gain.

CONCLUDING REMARKS

A real-time stability method was developed for stability analysis over a vehicle trajectory. The method is efficient and compatible with online calculations as well as for use with Monte Carlo analysis. The discovery was made that filtering the results and calculating error estimation provided measurements that were suitable for use in Monte Carlo analysis. The filtered results allowed a better means of obtaining a global minimum margin. The error estimation provided a means for flagging instances where the data were inconsistent.

Results from the real-time stability method compared well with results using frequency sweeps. Interpolation errors induced by coarser data caused the largest source of error. Simultaneously calculating the elevator and rudder margins can obtain a further increase in efficiency. Results obtained using simultaneous inputs compared well with results using separate inputs.

The real-time stability method works well for instances with reduced stability. The rudder loop gain was varied by as much as +8 dB. The real-time stability method produced a good calculated stability margin all the way to neutral stability. These data demonstrate that the real-time stability method can provide a good indication of an approaching instability.

The real-time stability method shows the potential to identify deficient instances in large Monte Carlo runs. This method is also compatible with real-time (online) applications.

Dryden Flight Research Center
National Aeronautics and Space Administration
Edwards, California, July 15, 2004

REFERENCES

1. Bosworth, J. T. and J. C. West, “Real-Time Open-Loop Frequency Response Analysis of Flight Test Data,” AIAA-86-9738, 1986.

2. Bosworth, John T. and John J. Burken, *Tailored Excitation for Multivariable Stability-Margin Measurement Applied to the X-31A Nonlinear Simulation*, NASA TM-113085, 1997.

3. Morelli, Eugene A., “Real-Time Parameter Estimation in the Frequency Domain,” AIAA Paper 99-4043, 1999.

4. Loe, Greg, Steve Munday, Jeremy Hart, and Scott Merkle, “X-38 Vehicle 131R Free Flights 1, 2 & 3: FCS & Aerodynamics Lessons Learned,” AAS 02-073, 2002.

5. Wacker, Roger, Dale Enns, Daniel Bugajski, Steve Munday, and Scott Merkle, “X-38 Application of Dynamic Inversion Flight Control,” AAS 01-016, 2001.

6. Flower, J. O., G. F. Knott, and S. C. Forge, “Application of Schroeder-Phased Harmonic Signals to Practical Identification,” *Journal of Measurement and Control*, Vol. 11, No. 2, February 1978, pp. 69–73.

REPORT DOCUMENTATION PAGE

Form Approved
OMB No. 0704-0188

1. REPORT DATE *(DD-MM-YYYY)*	2. REPORT TYPE	3. DATES COVERED *(From - To)*
10-02-2005	Technical Publication	

4. TITLE AND SUBTITLE
Real-Time Stability Margin Measurements for X-38 Robustness Analysis

5a. CONTRACT NUMBER

5b. GRANT NUMBER

5c. PROGRAM ELEMENT NUMBER

6. AUTHOR(S)
John T. Bosworth and Susan J. Stachowiak

5d. PROJECT NUMBER

5e. TASK NUMBER

5f. WORK UNIT NUMBER
953-50-00SE-RR-00-000

7. PERFORMING ORGANIZATION NAME(S) AND ADDRESS(ES)
NASA Dryden Flight Research Center
P.O. Box 273
Edwards, California 93523-0273

8. PERFORMING ORGANIZATION REPORT NUMBER
H-2565

9. SPONSORING/MONITORING AGENCY NAME(S) AND ADDRESS(ES)
National Aeronautics and Space Administration
Washington, DC 20546-0001

10. SPONSORING/MONITOR'S ACRONYM(S)
NASA

11. SPONSORING/MONITORING REPORT NUMBER
NASA/TP-2005-212856

12. DISTRIBUTION/AVAILABILITY STATEMENT
Unclassified -- Unlimited
Subject Category 08 Availability: NASA CASI (301) 621-0390

13. SUPPLEMENTARY NOTES
An electronic version can be found at the NASA Dryden Flight Research Center Web site, under Technical Reports.

14. ABSTRACT

A method has been developed for real-time stability margin measurement calculations. The method relies on a tailored-forced excitation targeted to a specific frequency range. Computation of the frequency response is matched to the specific frequencies contained in the excitation. A recursive Fourier transformation is used to make the method compatible with real-time calculation. The method was incorporated into the X-38 nonlinear simulation and applied to an X-38 robustness test. X-38 stability margins were calculated for different variations in aerodynamic and mass properties over the vehicle flight trajectory. The new method showed results comparable to more traditional stability analysis techniques, and at the same time, this new method provided coverage that is more complete and increased efficiency.

15. SUBJECT TERMS
Control, Excitation, Fourier, Margin, Stability

16. SECURITY CLASSIFICATION OF:			17. LIMITATION OF ABSTRACT	18. NUMBER OF PAGES	19a. NAME OF RESPONSIBLE PERSON
a. REPORT	b. ABSTRACT	c. THIS PAGE			STI Help Desk (email: help@sti.nasa.gov)
					19b. TELEPHONE NUMBER *(Include area code)*
U	U	U	UU	28	(301) 621-0390